BioTraffic: a bio-inspired behavioral model to vehicle traffic simulation

Carlos Eduardo Pereira de Quadros
Centro de Ciências Computacionais
Universidade Federal do Rio Grande
Rio Grande, Brazil
carlos.quadros@furg.br

Diana Francisca Adamatti
Centro de Ciências Computacionais
Universidade Federal do Rio Grande
Rio Grande, Brazil
dianaadamatti@furg.br

Alessandro de Lima Bicho
Centro de Ciências Computacionais
Universidade Federal do Rio Grande
Rio Grande, Brazil
albicho@furg.br

***Abstract*—This paper presents a new microscopic model to simulate the behavior of vehicle traffic through a bio-inspired agent-based method. The proposed model reinterprets a biologically-motivated method for generating leaf venation patterns in order to propose terrain reasoning, a technique that has been widely used in simulations and games. The main idea is to represent unoccupied spaces through abstract markers distributed in the environment. These markers identify free regions for the movement of vehicles in the simulated traffic environment. The markers provide space information and report the vehicular flow of the simulated scenario, including flow density and velocity. Typical behaviors observed in real traffic, including inhomogeneous driver models, lane changing and merging trajectories, are emergent properties of the proposed model. We demonstrate the flexibility and robustness of our model on simulation environments, comparing the statistical results with a commercial software used for traffic simulation.**

***Index Terms*—agent-based systems, terrain reasoning, traffic simulation, lane changing, lane merging, behavioral models**

I. Introduction

In general, the proposition of traffic simulation models requires considerable effort. However, the application of these models allows to reproduce computationally several situations of an analyzed context, providing predictive analysis of situations in a shorter time and with low costs [1]. In order to have a realistic traffic simulation model, it is important that the available information for the simulation is as close as possible to the real environment, because we do not have a robust model if this information does not correspond to reality. Several techniques for modeling traffic behavioral already exist [2], but important aspects have remained open for further research. Specifically, (i) the existing approaches are often focused on massive mathematical descriptions of traffic flows rather than usual (normal) behavior, in which drivers have goals to seek; (ii) existing traffic-modeling methods require careful parameter tuning to obtain visually convincing results; and (iii) the proposed models are limited to reproducing previously programmed behaviors, being inflexible to add new information on the roads.

This research proposes a novel traffic simulation model in virtual environments called *BioTraffic*. The main idea of this model is a bio-inspired agent-based method that occupies the simulation space basing on available markers in the environment. The proposed model is not a new *car-following*, but a different and innovative way to simulate the behavior of vehicles displacement in simulated environments. According to the principle of terrain reasoning, the markers are interpreted as available spaces for the displacement of vehicles in a simulation environment, providing information regarding the flow of vehicles on the road. The proposal is based on the *BioCrowds* model by Bicho et al. [3], which proposed a behavioral model for crowd simulation.

Therefore, the biologically-motivated method for generating leaf venation patterns by Runions et al. [4] is also reinterpreted to simulate vehicle traffic on roads. In the biological model, the simulated veins compete for access to sources of the plant hormone auxin, assumed to be distributed throughout the leaf blade. In our model, vehicles compete for space on the road, obtaining information about the flow density and velocity of the vehicles ahead. This information is obtained by analyzing the markers, which have similar purposes to auxins in the biological model. The agent-based approach is used because it allows to work with direct programming on each agent (microscopic model) and to analyze the results of simulations more broadly (such as macroscopic model). The implementation could be done directly in vehicle traffic simulation programs, but they do not have a test environment. In this way, we have also developed a specific agent-based simulator.

Based on a related literature review, it is not aware of a method to simulate vehicle traffic biologically inspired [2]. This unexpected analogy between methods used to simulate the development of leaf veins and to simulate the flow of vehicles on the road allowed us to propose a traffic model with few control parameters. The proposed model recreates emerging aspects of traffic simulation such as inhomogeneous driver models, lane changing and merging trajectories.

The rest of this paper is organized as follows: in Section II is presented the related works in the area. Section III presents the *BioCrowds* model, a bio-inspired crowd behavior model that motivated our research approach. Section IV provides the implementation of *BioTraffic* model. Section V are presented results and analysis investigated in the simulations. Finally, in Section VI we find the conclusions and future works.

II. Related Works

The analysis of the related works to traffic simulation was done from the perspective of three approaches: microscopic, macroscopic and mesoscopic models.

A. Microscopic Models

The model proposed by Nagel and Schreckenberg [5] is one of the most cited in the literature on traffic simulation. This work presents a stochastic car-following model to simulate traffic on a freeway through the use of cellular automata. The car-following model is one of the most used for the computational representation of vehicular traffic because of ease of use and flexibility in the re-adaptation of its parameters. The work of Brackstone and MacDonald [6] presents a review focused on several car-following models.

Lopez *et al.* [7] present the developments concerning intermodal traffic solutions, simulator coupling and model development and validation using SUMO (*Simulation Urban of MObility*). SUMO is an open-source, highly portable, microscopic and continuous traffic simulation package designed to handle large road networks [8]. Barria and Thajchayapong [9] present an algorithm for the detection and classification of anomalies in traffic simulation. Macedo *et al.* [10] present two versions of finite-state machine controllers to self-driving cars in the Simulated Car Racing Championship, a competition between controllers built on Open Racing Car Simulator (TORCS). A genetic algorithm was applied with default configurations found in the literature to evolve the controllers' parameters in the proposed models. Talebpour *et al.* [11] present a comprehensive simulation framework to model driver behavior in a connected driving environment with connected vehicles. Fountoulakis *et al.* [12] present a microscopic simulation investigation of a proposed methodology for highway traffic estimation with mixed traffic (connected and conventional vehicles). Lu *et al.* [13] present ten improvements for microscopic level interactions among classes of vehicles with varying levels of automation and connectivity. Menezes and Pozzer [14] present a model based on the steering behavior technique to develop a generic vehicle controller that guides the movement and behavior of vehicles inserted in a 3D world.

B. Macroscopic Models

Lighthill and Whitman [15] present a traffic simulation model adopting a kinematic wave method which was already used in supersonic projectile models and river flood movement. Kotsialos *et al.* [16] present a model for large-scale traffic flow. This work is focused on freeway networks using the METANET tool for validation. Helbing *et al.* [17] present a gas-kinetic ("Boltzmann-like") traffic equation for low and high vehicle densities. The model differs from others mainly by its non-local interaction term that takes into account the space requirements of vehicles and the correlations of successive vehicle velocities. Thonhofer *et al.* [18] present a modular macroscopic traffic model, using Partial Differential Equations (PDEs), with two traffic light formulations: an intersection approach that is a binary traffic light (detailed insights concerning queue length, flow across intersections and routing decisions can be investigated) and a continuous valve-like approach that allows investigation of averaged effects and large scale interaction and feedback effects. Lim *et al.* [19] present a stochastic motion planning algorithm and its application to traffic navigation that has been validated using simulations and real-world units using delay data collected from a set of taxis equipped with global positioning system sensors and a wireless network. Vallati *et al.* [20] present the urban traffic models for reducing congestion with a planning approach and a Planning Domain Definition Language (PDDL). Ngoduy and Jia [21] present how to derive a continuum traffic model considering both multiple forward and backward driving strategies. Spiliopoulou *et al.* [22] present a study that tests and compares different optimization algorithms employed to calibrate a macroscopic traffic flow model.

C. Mesoscopic Models

Using gas kinetics, Helbing *et al.* [23] present a new car-following model for traffic jam simulation, with an easy and intuitive calibration. Sewall *et al.* [24] propose a hybrid simulation technique that combines the strengths of two broad and different classes of traffic simulation to perform a flexible, interactive, and high fidelity simulation, even for large road networks. DynaMIT, proposed by Ben-Akiva *et al.* [25], is a real-time dynamic traffic assignment system that provides traffic predictions and travel guidance. This system contains two simulation tools: a Mesoscopic Demand Simulator and a Mesoscopic Supply Simulator. Burghout *et al.* [26] present a hybrid mesoscopic–microscopic model that applies microscopic simulation to areas of specific interest while simulating a large surrounding network in less detail with a mesoscopic model. Florian *et al.* [27] describe a simulation-based using an iterative dynamic equilibrium traffic assignment model. Potuzak [28] presents a Macroscopic-Simulation-Based Division (MaSBD) and the Microscopic-Simulation-Based Division (MiSBD) methods, which are both focused on a uniform load of the resulting sub-networks. Wilkie *et al.* [29] present a method for enhancing a road map from a *Geographic Information System* (GIS) database to create a geometrically and topologically consistent 3D model to be used in real-time traffic simulation, interactive visualization of virtual worlds, and autonomous vehicle navigation. Jamshidnejad *et al.* [30] present a framework to interface and integrate macroscopic flow models and microscopic emission models. Burghout and Koutsopoulos [31] present a framework for implementing hybrid models that facilitate consistent representation of traffic dynamics.

D. Summarization of Related Works

The basis for the related works was concentrated in the search for papers with the term "traffic simulation", which has one of the following terms: microscopic, macroscopic and/or mesoscopic.

Table I presents the summarization of the related works, selected by relevance in the area or most current works. In this table, we present our approach in the last line to have parameters for further comparisons.

III. BioCrowds Model

The model was originally proposed by Runions *et al.* [4] to model the development of veins of plant leaves and tree branches by disputing a plant hormone called "auxin". That work presents a potential application in several areas of research because its main idea is the contest for free space. Based on this biological model, Bicho *et al.* [3] proposed a model called *BioCrowds*, to simulate the crowds' dynamics where each agent contests space using available markers as resources in the environment, to avoid collision with other agents or obstacles in scenarios, to reach the desired location. In our work, we follow the same reasoning, which proposes a new microscopic model for vehicle traffic in a virtual environment called *BioTraffic*.

A. Calculation for agent movement and orientation – BioCrowds and BioTraffic

Each time, the agent i moves in the simulation. It is necessary to update its position $\boldsymbol{p}(t)$ and, consequently, the target vector $\boldsymbol{g}(t)$ (agent destination point in the simulation scenario). The set S contains all the markers close to agent i in the simulation scenario. These markers are part of the "perception area", where $S = \{a_1, a_2, ..., a_N\}$. The set of N markers linked to agent i in $S = \{\boldsymbol{a}_1, \boldsymbol{a}_2, ..., \boldsymbol{a}_N\}$. Therefore, to calculate the next step of agent i and obtain a new position, we use a set of vectors $S' = \{\boldsymbol{d}_1, \boldsymbol{d}_2, ..., \boldsymbol{d}_N\}$, where:

$$\boldsymbol{d}_k = \boldsymbol{a}_k - \boldsymbol{p}, \tag{1}$$

considering the position $\boldsymbol{p}$ of the agent and the markers in S (markers in the perception area - Fig. 1).

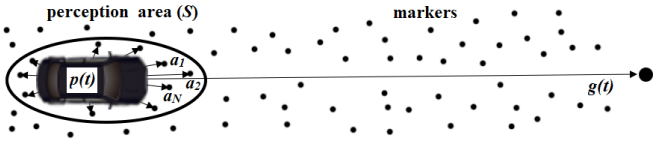

Fig. 1. Calculation for agent movement and orientation considering the markers in the simulated scenario.

In a second moment, the generation of "vein patterns" (term used to the plant vein generation model), the vectors in S' are normalized and added, resulting in orientation to the vein growth. In the simulation of the displacement of an agent, it is also necessary to consider its destination ($\boldsymbol{g}$ target vector). Therefore, for each $\boldsymbol{d}$ $vector \in S'$ has assigned a weight relative to its alignment with the target agent vector. In other words, it is the angle between the vectors. Specifically, the $\boldsymbol{m}$ motion vector is:

$$\boldsymbol{m} = \sum_{k=1}^{N} w_k \boldsymbol{d}_k, \tag{2}$$

where the w_k coefficients are the weights, calculated through equation:

$$w_k = \frac{f(\boldsymbol{g}, \boldsymbol{d}_k)}{\sum_{l=1}^{N} f(\boldsymbol{g}, \boldsymbol{d}_l)}. \tag{3}$$

To determine function f, let us first assume that all markers $\boldsymbol{a}_k$ affecting agent i are at the same distance $\|\boldsymbol{d}_k\|$ from this agent. Such function should:

- reach its maximum when the (nondirected) angle θ between $\boldsymbol{g}$ and $\boldsymbol{d}$ is equal to $0°$;
- reach its minimum when $\theta = 180°$;
- decrease monotonically as θ increases from $0°$ to $180°$; and
- variables must have values greater than or equal to zero.

A possible choice for f is

$$f(\boldsymbol{g}, \boldsymbol{d}_k) = \begin{cases} \dfrac{1 + \cos\theta}{1 + \|\boldsymbol{d}_k\|}, & \text{se} \quad \|\boldsymbol{d}_k\| > 0 \\ 0, & \text{se} \quad \|\boldsymbol{d}_k\| = 0, \end{cases} \tag{4}$$

where

$$\cos\theta = \frac{\langle \boldsymbol{g}, \boldsymbol{d}_k \rangle}{\|\boldsymbol{g}\| \|\boldsymbol{d}_k\|}. \tag{5}$$

Equation (2) presents vector $\boldsymbol{m}$ responsible for the agent movement from its origin to its destination. During the route, when space is available, the model allows the agent to move with a desired maximum speed $s_{\max}$.

Regarding space availability, when the agent runs through denser places with less availability of markers and an excessive number of agents or obstacles, its speed is reduced. For this, the model needs to adjust the displacement velocity of the agent, according to the $\boldsymbol{m}$ vector modulus and the $s_{\max}$ value. The instantaneous motion vector, in displacement units by position change (each iteration), $\boldsymbol{v}$, is given by $\boldsymbol{v} = s_{\min} \frac{\boldsymbol{m}}{\|\boldsymbol{m}\|}$, where:

$$s_{\min} = \min\left\{\|\boldsymbol{m}\|, s_{\max}\right\}. \tag{6}$$

In (6), $\|\boldsymbol{m}\| > s_{\max}$ (maximum agent displacement) is limited for $s_{\max}$. Otherwise, the displacement is given by $\|\boldsymbol{m}\|$.

IV. BioTraffic Model

Firstly, we verify how the *BioCrowds* markers could be included in the proposal to develop a behavioral model for agents whose geometry and properties are in a two-dimensional vehicle. In crowd simulation, each agent, in order to arrive at the desired location, contests space using markers as a resource available in the environment, avoiding to collide with other agents and obstacles in the enviroment. In this way, in *BioTraffic*, this feature has the same properties and it provides further information that will be detailed in the sequence.

In both models, the distance between markers plays a key role in two important aspects of the simulation: computational cost and realism in the agents' movement. With that, the larger

TABLE I
SUMMARY OF THE MAIN MICROSCOPIC, MACROSCOPIC AND MESOSCOPIC MODELS CITED ON THE RELATED WORKS.

Authors	Type	Techniques	Results
Lighthill and Whitham [15]	Macro	Kinematic wave method	A theory of the propagation of changes in traffic distribution along of roads.
Nagel and Schreckenberg [5]	Micro	Cellular automata	Simulate traffic on a freeway.
Helbing *et al.* [23]	Meso	Gas-kinetic-based and car-following	Combine micro/macro simulations of road sections by simple algorithms.
Jamshidnejad *et al.* [30]	Meso	Car-following and emission models	A new mesoscopic integrated flow-emission model that balances the trade-off between high accuracy and low computation time.
Lopez *et al.* [7]	Micro	Car-following	Introduce SUMO as a large framework with helpful tools for the generation, validation and evaluation of large traffic scenarios.
Thonhofer *et al.* [18]	Macro	Discretization of PDEs	Present a modular macroscopic traffic model with two traffic light formulations.
Our approach	Micro	Multiagent system	Agent-based approach, reproducing emerging behaviors in multi-lane traffic.

the number of markers per area, the greater the smoothness of the agents' movement. However, the computational cost is higher.

In order to represent the movement carried out by the vehicles and their respective restrictions, the *BioTraffic* proposal is based on a model widely used on autonomous vehicles, the *Ackermann Steering Geometry* model [32] (Fig. 2). This model has the following parameters: ICR (*Instantaneous Center of Rotation*) represents the external reference point that serves as the basis for the vehicle to perform the rotation; TR (*Turning Radius*) is a midpoint between the wheels of the rear of the vehicle; SWA (*Steering Wheel Angle*) regulates the steering angle; and L (*Length*) refers to the length of the vehicle, particularly the distance between the axles (front and rear).

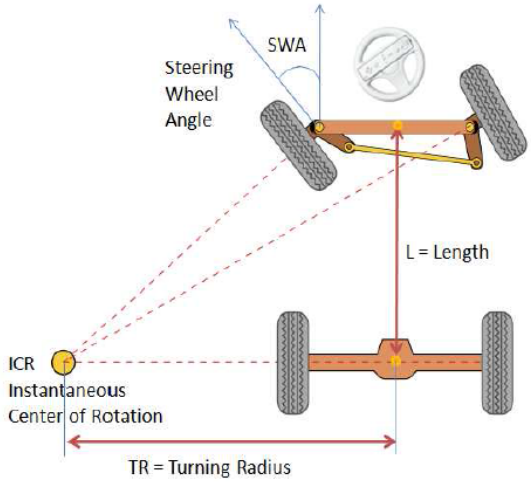

Fig. 2. Ackermann steering geometry model (adapted from [33]).

The ICR aims to provide an external reference point for orientation, and later collaborate with the directional calculations with the other points in the vehicle. The ICR aligned horizontally to the median point on the rear axle from the TR. With this alignment, we have precision for the radius size that will be formed when the vehicle performs some kind of maneuver in its direction. In the model, the size of the bar linking the two axes (front and rear) also influences the size of the radius. Small vehicles will occupy less space when making a left turn, for example. On the other hand, vehicles with a larger bar will need more space to make directional maneuvers. At last, we have the SWA which varies according to the dimensions of TR and L, according to the following equality $SWA = \arctan(\frac{L}{TR})$.

The general idea of the *Ackermann* model was reinterpreted by calculating the SWA angle, which informs the maximum angular variation of the left or right orientation of the vehicle. We adopted it in *BioTraffic* model, with a perception angle of the markers corresponding to $2SWA$, and it would produce the same directional effect in the vehicle (hatched area in Fig. 3).

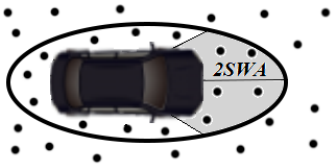

Fig. 3. Perception angle agent of the markers corresponding to $2SWA$.

When moving, the agent (vehicle) realizes a variation in the orientation that produces noise in its trajectory, i.e., unnecessary orientation movements concerning its objective. In order to reduce this noise in the orientation, the weighted moving average was implemented, through:

$$\boldsymbol{g} = w\boldsymbol{g} + (1 - w)\boldsymbol{m_{ant}}, \tag{7}$$

where $\boldsymbol{g}$ is the target vector, $\boldsymbol{m_{ant}}$ is the previous orientation of the agent, and w is the normalized weighting factor of the equation [34].

A. Agent Orientation Calculation

The markers not only inform a spatial reference scenario. An approach that integrates the concept of terrain reasoning

to *BioCrowds* model was proposed in [35], where the markers serve not only as a spatial reference in the simulated environment to calculate the orientation of the agents, but also other attributes that help to differentiate areas within the environment. In [35], markers identify three possible route regions on the ground: walkable, preferably non-walkable, and non-walkable. The terrain features are created through an algorithm that provides different weights for each different region.

In *BioTraffic* model, the terrain reasoning is used to calculate the agents' speed in vehicle traffic simulator, but with a different approach defined in the methodology proposed by [35]. The markers inform, through one of their attributes (by a variable called *service capability*), the current maximum traffic lane speed. This information is adopted for calculating the vehicle's travel speed, and it is relative to the lane that is permitted in accordance with the maximum speed limit previously set for the vehicular lane or the current flow. In addition, to this information relating to the speed, the markers remain with geometric reference to calculate the displacement agent.

The markers inform the displacement availability of the agents, i.e., the spatial coordinates are used to calculate the sum vector of the direction vectors obtained from each marker contained in the personal space of the agent (vehicle). Equation (1), which computes the direction vectors; Equation (2), which finds the movement vector; and Equation (3), which weights each vector in relation of the set of direction vectors, are adopted in *BioTraffic* as well as they are applied in *BioCrowds*.

Regarding the angular variation of the orientation, the vehicle model must be restrictive due to the form of movement and orientation is each agent (vehicle). In *BioCrowds*, when a pedestrian finds obstacle, s/he can make a turn of up to 90^0 or more, to deviate from it and try to reach his/her goal. However, the smaller the deviation angle, the better the displacement considering the principle of least effort. For vehicles, the constraint is greater and limited by a vehicular attribute called the *angle of rotation*. According to the *Ackermann* model, turning angle takes into account vehicle size (particularly the distance between the extreme axles) and the same turning diameter.

B. Agent Speed Calculation

When analyzing computational tools of traffic simulation of vehicles, we realize that the majority adopts the car-following model. This is used to simulate an essential part in getting traffic engineering results: the displacement of vehicles in the environment.

The markers in the area of agent space perception will form a set that defines the perimeter in which they are within reach of the agent. These, in turn, are used at the moment in which the displacement is occurring, passing information about orientation and speed for the agents. After being used, they are available for contesting between the nearby agents. The agent only finishes its movement when it finds its goal, i.e., where there are no more markers to be contested in the path between the beginning and the end of its route.

In relation to space in the *BioTraffic* model, the "association" of the labels with the agents is performed from the agents, differently of *BioCrowds* model, whose "association" is performed from the labels in themselves. To ensure that the agent is the closest to the correct label, each label has a variable that identifies which agent is using it. During the partitioning process performed at each t instant of simulation, a marker could be associated with different agents at different t times. However, at the end of the process, only the nearest agent is effectively associated with one specific marker. Therefore, during the displacement of vehicles from the destination source, each used marker has its agent identification variable.

The movement of each agent is calculated iteratively. The position $\boldsymbol{p}(t)$ and the target vector $\boldsymbol{g}(t)$ are calculated at each simulation step. The markers contained in the agent's "personal space" will be stored in set S. The *service capacity* variable will be used to calculate the movement speed of vehicles in relation to what is allowed in the lane.

The *service capacity*, an attribute associated with each marker which informs the current maximum traffic lane speed, has its value changed after the agent adjusts its speed according to this attribute value. After, the attribute is changed to the updated speed value of the agent, which may be the value previously reported by this same marker or a lower value. The updated speed information is used for the next vehicles in the lane. In this way, the current speed record of the last agent that passed that marker is stored.

Initially, the average service capacity velocity $\bar{vel}_{\text{capacity}}$ of all markers in set S is calculated as follows:

$$\bar{vel}_{\text{capacity}} = \frac{\sum_{k=1}^{N} vel_{\text{capacity}_k}}{N}, \tag{8}$$

and it is defined as $vel_{\text{ref}} = \bar{vel}_{\text{capacity}}$.

This average velocity will be compared to the limit speed defined for each agent, called vel_{lim}, determining the reference velocity for the agent, called vel_{ref}:

$$vel_{\text{ref}} = \begin{cases} vel_{\text{lim}}, & \text{if} \quad vel_{\text{lim}} < vel_{\text{ref}} \\ vel_{\text{ref}}, & \text{otherwise.} \end{cases} \tag{9}$$

From the definition of this reference velocity, it is possible to verify what the reference acceleration of the agent should be, called $acel_{\text{ref}}$, using vel_{ref} and the defined limit acceleration for each agent, called $acel_{\text{lim}}$. For that, each agent has a variable that informs its current speed called vel. In this way, the agent acceleration is initially calculated by uniformly variable rectilinear motion:

$$acel_{\text{ref}} = \frac{vel_{\text{ref}} - vel}{t}. \tag{10}$$

Subsequently, it is compared with the defined limit acceleration of each agent:

$$acel_{\text{ref}} = \begin{cases} acel_{\text{lim}}, & \text{if} \quad acel_{\text{lim}} < acel_{\text{ref}} \\ acel_{\text{ref}}, & \text{otherwise.} \end{cases} \tag{11}$$

After, we obtain the reference displacement of the agent, according to the reference acceleration, at simulation time t:

$$s_{\text{ref}} = vel.t + \frac{acel_{\text{ref}}.t^2}{2}. \quad (12)$$

Note that the reference displacement s_{ref} has the same purpose of variable $s_{\max}$ in (6). Equation (13) calculates, for the instantaneous movement vector, in displacement units by position change (each iteration) $\boldsymbol{v} = s_{\min}\frac{\boldsymbol{m}}{\|\boldsymbol{m}\|}$, where:

$$s_{\min} = \min\{\|\boldsymbol{m}\|, s_{\text{ref}}\}. \quad (13)$$

In (13), case $\|\boldsymbol{m}\| > s_{\text{ref}}$, the maximum displacement of the agent is limited by s_{ref}. Otherwise, the displacement is given by $\|\boldsymbol{m}\|$.

Finally, the value of the variable vel is updated according to the Torricelli equation:

$$vel = \sqrt{vel^2 + 2.acel_{\text{ref}}.\|\boldsymbol{v}\|}. \quad (14)$$

After that, the agent is moved. For that, it is necessary to update the *service capability* attribute of the markers that were associated with the agent. From the markers set in the set S of the agent, only those that are behind, considering its orientation, will have their service capacity values updated.

In order to be able to select the markers behind the agent, its orientation vector was momentarily changed to its opposite, i.e., with the same modulus, same direction, but opposite direction. Afterward, the in-cone function selected a subgroup of the markers, adopting as parameters the radius of the individual space of the agent and an angle that varies according to the number of lanes. In this work, the angle values adopted were 180^0 in the simulations of a single lane, and $2.arctan(2/R)$, in the simulations with two lanes, considering the track width equal to $4m$ and the radius of perception R.

Algorithm 1 describes the *BioTraffic* model for simulating vehicle traffic.

Algorithm 1: Algorithm for Vehicle Traffic Simulation - *BioTraffic* model

Require: $agents[vel, vel_{\text{lim}}, a_{\text{lim}}, R \geq 0, g], S, step$
Ensure: $agents$
repeat
  for *each agent* i **do**
    $S_i = \varnothing$
  end for
  for $\boldsymbol{a} \in S$ **do**
    $incrementalTest\_servCapability(\boldsymbol{a}, step)$
    $i = closestAgent(\boldsymbol{a})$
    if $distance(\boldsymbol{p}_i, \boldsymbol{a}) \leq R_i$ **then**
      $S_i = S_i \cup \{\boldsymbol{a}\}$
    end if
  end for
  for *each agent* i **do**
    if $S_i \neq \varnothing$ **then**
      $S_i' = \{\boldsymbol{d} \mid \boldsymbol{a} \in S_i, \boldsymbol{d} = \boldsymbol{a} - \boldsymbol{p}_i\}$
      $\boldsymbol{m}_i = \sum_{\boldsymbol{d} \in S_i'} w\boldsymbol{d},\ where\ w = f(\boldsymbol{g}_i, \boldsymbol{d}) / \sum_{\boldsymbol{d}' \in S_i'} f(\boldsymbol{g}_i, \boldsymbol{d}')$
      $vel_{\text{ref}} = \sum_{\boldsymbol{a} \in S_i} servCapability(\boldsymbol{a})$
      $vel_{\text{ref}} = vel_{\text{ref}} / \| S_i \|$
      if $vel_{\text{lim}} < vel_{\text{ref}}$ **then**
        $vel_{\text{ref}} = vel_{\text{lim}}$
      end if
      $a_{\text{ref}} = (vel_{\text{ref}} - vel)/t$
      if $a_{\text{lim}} < a_{\text{ref}}$ **then**
        $a_{\text{ref}} = a_{\text{lim}}$
      end if
      $s_{\text{ref}} = vel.t + a_{\text{ref}}.t^2/2$
      $\boldsymbol{v}_i = (\boldsymbol{m}_i / \|\boldsymbol{m}_i\|) s_{\min},\ where\ s_{\min} = \min\{\|\boldsymbol{m}_i\|, s_{\text{ref}}\}$
      $\boldsymbol{p}_i^{old} = \boldsymbol{p}_i$
      $\boldsymbol{p}_i = \boldsymbol{p}_i + \boldsymbol{v}_i$
      $vel = \sqrt{vel^2 + 2.a_{\text{ref}}.\|\boldsymbol{v}_i\|}$
      $update\_servCapability(p_i^{old}, g, S_i, vel)$
    end if
  end for
until *finished simulation*

V. Results and Analysis

This section presents the results after the simulations and their analysis.

A. Used Tools

In work [36], the authors presented comparisons between simulation tools to traffic simulation software. For our development, we choose the NetLogo tool[1], because it is a programmable modeling environment of natural and social phenomena widely used in the area of agent-based systems [37]. It has a significant number of models implemented in many areas, such as arts, biology, chemistry, physics, computer science, natural sciences, economics, social sciences, and mathematics.

During the analysis of other tools, the most similar to our approach was Aimsun (*Aimsun traffic modelling software*)[2], developed by Transport Simulation Systems - TSS. It presented the best usability and practicality for the construction of the simulation scenarios, control over vehicle demands, addition of different modes and validation of results [38].

Aimsun stands out for the exceptionally high speed of its simulations and for fusing travel demand modeling, static and dynamic traffic assignment with mesoscopic, microscopic and hybrid simulation - all within a single software application. The following car model used in Aimsun refers to the GIPPS model [39]. The model development is not based on global parameters, but on parameters of each type of driver (speed limit, vehicle acceptance), the geometry of each section (speed limit in curves and others) and the influence of vehicles in adjacent lanes [38]. With this, the work constructs a new model

[1] https://ccl.northwestern.edu/netlogo/
[2] www.aimsun.com

for response to vehicle followers, based on the parameters' definition of each vehicle, such as its acceleration rates.

In our model, the input flow generation on the lane was implemented in the same way as Aimsun. The dimensions of both the agents and the environment were adapted to the same scale.

B. Environment Configuration Parameters in NetLogo

The environment for the configuration is divided into *patches*, defining that each unit represents $1m^2$. The shapes editor, available in NetLogo, features four quadrants containing 10x10 small squares each. The size of the agent's form in the editor does not exceed the size value of one *patch*[3]. However, by entering the edited form, it is possible to scale the agent's size according to the average vehicle's length. The vehicle shape was defined as a length equal to 19/20 quadrilaterals of the editor. This proportionality factor is used when scaling the shape to the means of the calculated lengths.

The adaptation analysis of the vehicle traffic model in relation to the crowds model has a restriction about the direction change movement of the vehicles, when compared to the human movement. When initiating the simulation, with no angular constraint, the vehicle should make a 90^0 spin on its centroid and proceed to the objective (straight line shown in Fig. 4), since this is the expected behavior of a virtual human in a simulator. In the same figure, it is possible to see a trace left by the vehicle (semicircle connected to the straight line). It made the rotation according to the angular constraint imposed by the implementation done in *BioTraffic*. In this way, Fig. 4 presents both displacements, where the straight line refers to human displacement, and the half-circle refers to the displacement of a vehicle.

Fig. 4. Final direction and orientation of a vehicle without the Ackermann method implemented in *BioTraffic*.

C. Comparison with Aimsun simulator

The validation of the developed model was performed comparing Aimsun traffic simulator results, a commercial simulator. The values of Table II were the same set in both simulators (Aimsun and *BioTraffic*).

After defining the data input configurations through the *BioTraffic* simulator interface (Fig. 5), 10 (ten) simulations were performed in the *NetLogo*, because the developed model presents dynamic results (random input of vehicles). In the same way, the experiments were carried out in Aimsun that presents static results. After that, the average of the results between each simulator and the comparison of the results were calculated. The simulation time was 5 minutes (Table II).

[3]Spatial unit in NetLogo language.

TABLE II
AIMSUN AND BIOTRAFFIC INPUT PARAMETERS.

Input	Values	Units
Lane number	2	units
Lane type	freeway	none
Maximum speed per lane	120	km/h
Lane bandwidth	3.5	m
Lane length	1	km
Vehicle lenght	4	m
Vehicle aceleration	3	m/s^2
Vehicle limit speed	110	km/h
Traffic flow	3600	vph
Simulation time	5	min
Data collection time	1	min

The data obtained in each minute presented 60 vehicles in each one. Multiplying by 5 minutes, the values obtained by the total time of simulation, we have 300 vehicles in the total, for each experiment. In the configuration of the Aimsun traffic state, it was indicated that it would receive an inflow of 3600 vehicles per hour (vph). Therefore, by multiplying the flow of a five-minute experiment by twelve hours (considering full hour), we have the same 3600 vehicles per hour.

As presented in Fig. 6, *BioTraffic* had an average input flow of 291 vehicles, being close to the ideal flow as compared to the Aimsun simulator. Using the same calculation to check the flow per hour, the model has a flow of 3492 per hour. In the first collection of *BioTraffic*, 59 vehicles were presented and in the others, 58 vehicles. When initiating a simulation, there is a need to add an agent in the simulation environment. Therefore, the entry difference of vehicles between the two simulators is two vehicles at each data collection.

Fig. 7 represents the comparison of the average between vehicle densities of the experiments performed. In the first moment, *BioTraffic* presents a higher density, compared to the first minute of the Aimsun, that stabilizes in a few minutes. The results of the simulation of both are equivalent (before the second minute), where the simulator Aimsun continues to increase its density until the third minute.

Fig. 8 shows an oscillation in the travel simulator values of the Aimsun, after the first minute, comparing to *BioTraffic*. Even if they are close, the results do not present the same behavior, because our model does not have a balance of distribution of the values for the speed of the vehicles during the simulation. In Aimsun, even if a vehicle is alone on the road, the driving speed is not constant, unlike in *BioTraffic*.

Fig. 9 presents the highest average speed between vehicles only at the end of the simulation to Aimsun. In *BioTraffic*, the speed, in the first minute, is 107 km/h. As the displacement process is given by the space contest in the simulated environment, the speed of the vehicles automatically decreases during the route. Meanwhile, the Aimsun shows some oscillations during the process. The velocities of both simulations approximate just at the end of the experiment. All

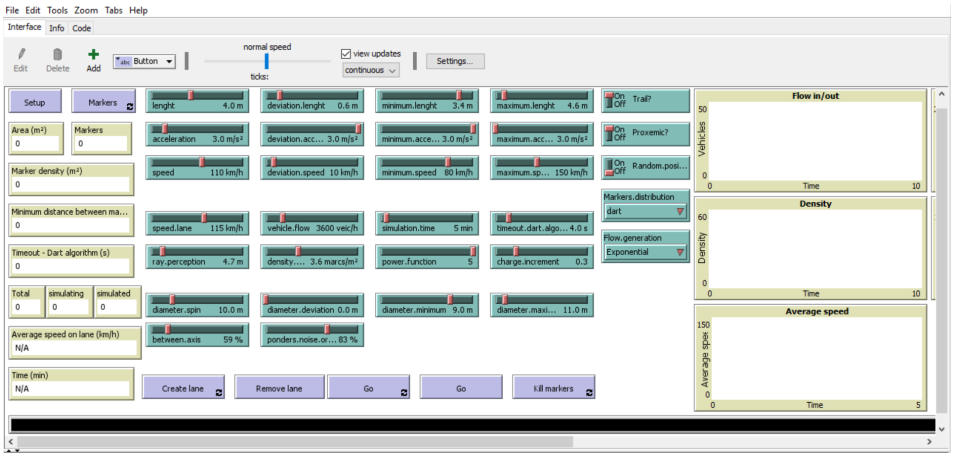

Fig. 5. *BioTraffic* simulator interface.

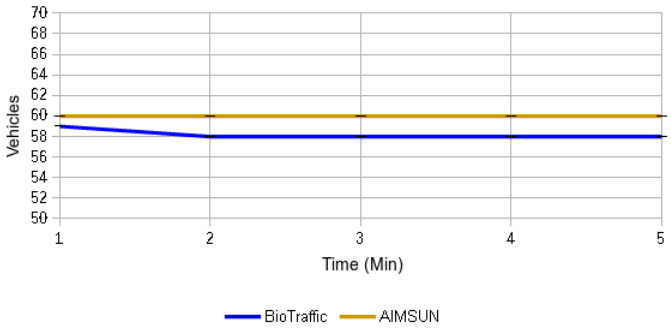

Fig. 6. Vehicles input flow per lane.

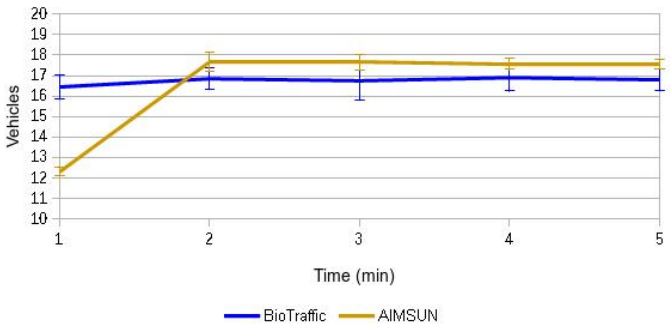

Fig. 7. Vehicles density in lane.

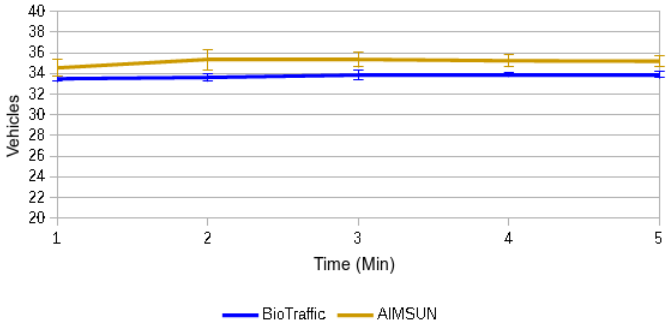

Fig. 8. Vehicles travel time during simulation.

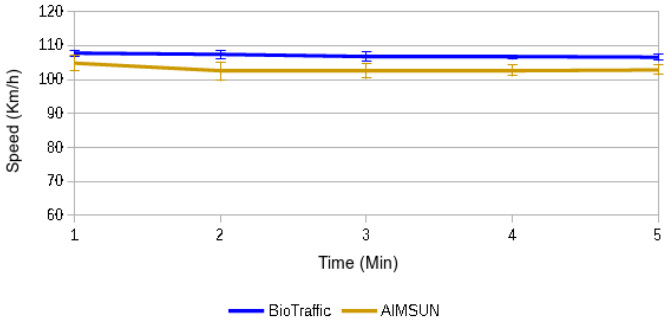

Fig. 9. Vehicles average velocity in line.

BioTraffic averages are above 105 km/h. Whilst Aimsun, in most data, kept the average speed below this value.

There is a series of data for calibration in Aimsun, in addition to those presented here during the results obtained. Just in the vehicle class, for simulations with dynamic models, we must calibrate the following items: speed acceptance, the minimum distance between vehicles, maximum preference time, acceptance of being guided, reaction time, reaction to the vehicle of the front, deceleration, sensitivity factor, minimum headway, percentage of overtaking, and so on. However, these data do not influence the comparison data in this work, because the *BioTraffic* simulator has fewer data to calibrate.

D. *Emerging behaviors*

In this section we present examples that illustrate features of the proposed method. In terms of simulating realistic traffic, lane changing and merging behaviors are important features in multi-lane simulations. When a vehicle changes lanes from one lane to another, this can have the effect of a wave slowing both lanes. Similarly, the merging of two lanes may produce a reduction in capacity due to the generated bottleneck. Bot-

tlenecks are result of a specific physical condition, often the design of the road, but they can also be caused by temporary situations, such as vehicular accidents.

In the proposed model, unlike the methods proposed in the literature, readily emerge in our simulations, as it can be visually observed in Fig. 10. Because the algorithm is based on competition for space, lane changing emerge due to the driver's intention to keep his/her speed. In frame sequence in the figure, it is possible to verify the exchange of lanes under the same conditions by drivers identified by "A" and "B". In order to understand whether the driver is accelerating, decelerating or maintaining his/her speed, the colors green, red and blue were adopted. It is possible to analyze that driver "A" when starting the maneuver reduced and maintained speed until completing the lane change. However, the driver "B" kept his/her speed checked during the same maneuver.

In Fig. 11 an accident was simulated, in order to reproduce the lane merging. The behavior is reproduced by the proposed model, just that the damaged vehicles remain with their markers. Consequently, the two lanes are reduced to a single one, and drivers compete for the space available on the way.

VI. Conclusions

This paper proposes a new model named *BioTraffic* to determine how vehicles move in the simulation environment. Vehicles compete for space from origin to destination using available markers along the way. According to the principle of terrain reasoning, the markers are interpreted as spaces available for the displacement of vehicles, and provide information regarding the flow of vehicles on the road.

Through analyzing the data obtained from the model simulations and Aimsun simulator, it was verified that the proposed model presented results corresponding to those of the vehicle traffic simulator. It should be noted that the simulator used in the validations of the results has a number of parameters that were not adopted in our model, making our proposal more straightforward and with results very close to a commercial simulator. Regarding visual results, the method reproduces characteristic behaviors in multi-lane traffic - lane changing and merging behaviors - due to the principle of space competition, an idea originally adopted by the biological model.

The terrain reasoning became a possible way of understanding how agents can map a displacement without the need for direct interaction with other agents in the environment. In the model proposed in this paper, interaction occurs through shared space, rather than between agents. The ability to move a vehicle on *BioTraffic* does not depend on a road or the presence of another vehicle in the simulation.

BioTraffic is different from the more conventional model widely used because it has the capacity for new types of simulation, the interaction of the agent is made with the environment and not with the other agents, the scenarios do not need lanes to control the queues. In other words, vehicles travel freely from the source to their destination, disputing available resources along the way. This model is more complex than the car-following, because it has a richness in the refinement of movements and the effective use of the displacement space are different from models in which only "cars follow cars".

In future works, we will improve the terrain reasoning, where the service capabilities would have different weights in the markers. In this way, it would be possible to identify lanes with different flows (double-hand lanes), to adopt a greater weight of relevance for markers that would serve to overtake, for example. We also intend to propose improvements to the model by adding georeferenced data from open maps, such as OpenStreetMap[4], and implementing parallel processing techniques on GPUs (Graphics Processing Units).

Acknowledgment

Authors would like to thank Brazilian Agency FAPERGS for funding (ARD 11/1788-0), and Dr. Hélida Salles Santos for reviewing this work.

References

[1] R. P. Roess, E. S. Prassas, and W. R. McShane, *Traffic Engineering*, 4th ed. United States: Prentice Hall/Pearson, 2011.

[2] Q. Chao, H. Bi, W. Li, T. Mao, Z. Wang, M. C. Lin, and Z. Deng, "A survey on visual traffic simulation: Models, evaluations, and applications in autonomous driving," *Computer Graphics Forum*, vol. 39, no. 1, pp. 287–308, 2020.

[3] A. de Lima Bicho, R. A. Rodrigues, S. R. Musse, C. R. Jung, M. Paravisi, and L. P. Magalhaes, "Simulating crowds based on a space colonization algorithm," *Computers & Graphics*, vol. 36, no. 2, pp. 70 – 79, 2012.

[4] A. Runions, B. Lane, and P. Prusinkiewicz, "Modeling trees with a space colonization algorithm," in *Proceedings of the Third Eurographics Conference on Natural Phenomena*, ser. NPH'07. Aire-la-Ville, Switzerland, Switzerland: Eurographics Association, 2007, pp. 63–70.

[5] K. Nagel and M. Schreckenberg, "A cellular automaton model for freeway traffic," *J. Phys. I France*, vol. 2, no. 12, pp. 2221 – 2229, December 1992.

[6] M. Brackstone and M. McDonald, "Car-following: a historical review," *Transp. Research Part F: Traffic Psychology and Behaviour*, vol. 2, no. 4, pp. 181 – 196, 1999.

[7] P. A. Lopez, M. Behrisch, L. Bieker-Walz, J. Erdmann, Y.-P. Flötteröd, R. Hilbrich, L. Lücken, J. Rummel, P. Wagner, and E. WieBner, "Microscopic traffic simulation using sumo," in *2018 21st International Conference on Intelligent Transp. Systems (ITSC)*. IEEE, 2018, pp. 2575–2582.

[8] D. Krajzewicz, J. Erdmann, M. Behrisch, and L. Bieker, "Recent development and applications of SUMO - Simulation of Urban MObility," *International Journal On Advances in Systems and Measurements*, vol. 5, no. 3&4, pp. 128–138, December 2012.

[9] J. A. Barria and S. Thajchayapong, "Detection and classification of traffic anomalies using microscopic traffic variables," *IEEE Transactions on Intelligent Transp. Systems*, vol. 12, no. 3, pp. 695–704, Sept 2011.

[10] B. H. F. Macedo, G. F. P. Araujo, G. S. Silva, M. C. Crestani, Y. B. Galli, and G. N. Ramos, "Evolving finite-state machines controllers for the simulated car racing championship," in *14th Brazilian Symposium on Computer Games and Digital Entertainment*, Piaui, Brazil, November 2015, pp. 160–172.

[11] A. Talebpour, H. S. Mahmassani, and F. E. Bustamante, "Modeling driver behavior in a connected environment: Integrated microscopic simulation of traffic and mobile wireless telecommunication systems," *Transp. Research Record*, vol. 2560, no. 1, pp. 75–86, 2016.

[12] M. Fountoulakis, N. Bekiaris-Liberis, C. Roncoli, I. Papamichail, and M. Papageorgiou, "Highway traffic state estimation with mixed connected and conventional vehicles: Microscopic simulation-based testing," *Transp. Research Part C: Emerging Technol.*, vol. 78, pp. 13–33, 2017.

[13] X.-Y. Lu, X. D. Kan, S. E. Shladover, D. Wei, and R. A. Ferlis, "An enhanced microscopic traffic simulation model for application to connected automated vehicles," in *96th Annual Meeting of the Transp. Research Board, Washington, DC*, 2017.

[4] https://www.openstreetmap.org

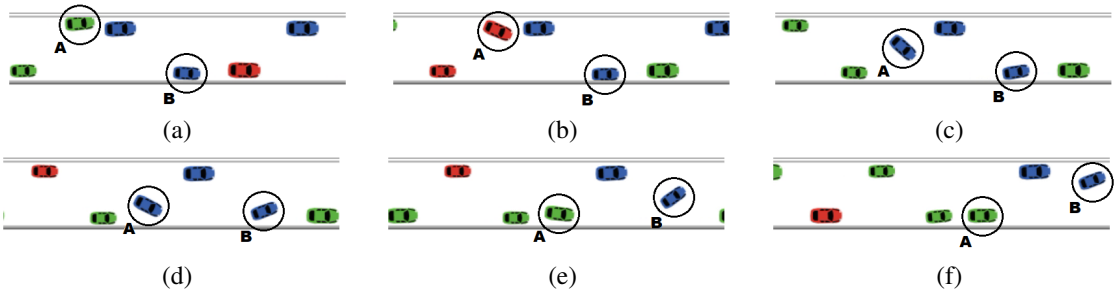

Fig. 10. Snapshots of lane changing maneuvers performed by two drivers.

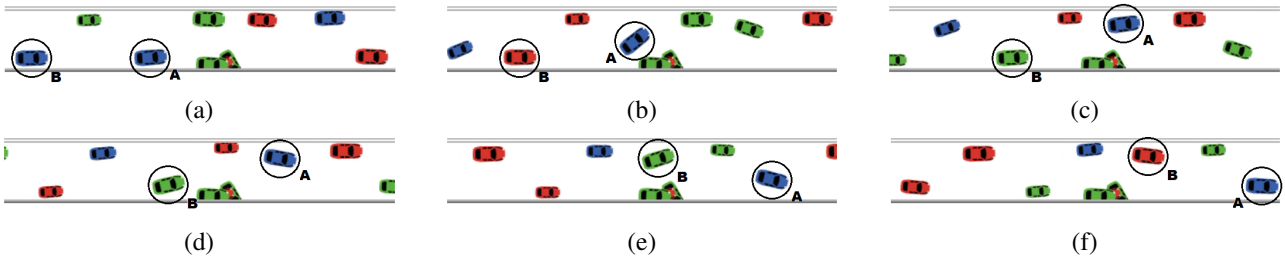

Fig. 11. Snapshots of lane merging maneuvers performed by two drivers.

[14] V. P. Menezes and C. T. Pozzer, "Development of an autonomous vehicle controller for simulation environments," in *17th Brazilian Symposium on Computer Games and Digital Entertainment*, Foz do Iguaçu, Brazil, October 2018, pp. 75–80.

[15] M. J. Lighthill and G. B. Whitham, "On kinematic waves. ii. a theory of traffic flow on long crowded roads," *Proceedings of the Royal Society of London A: Mathematical, Physical and Engineering Sciences*, vol. 229, no. 1178, pp. 317–345, 1955.

[16] A. Kotsialos, M. Papageorgiou, C. Diakaki, Y. Pavlis, and F. Middelham, "Traffic flow modeling of large-scale motorway networks using the macroscopic modeling tool metanet," *IEEE Transactions on Intelligent Transp. Systems*, vol. 3, no. 4, pp. 282–292, Dec 2002.

[17] D. Helbing, A. Hennecke, V. Shvetsov, and M. Treiber, "Master: macroscopic traffic simulation based on a gas-kinetic, non-local traffic model," *Transp. Research Part B: Methodological*, vol. 35, no. 2, pp. 183–211, 2001.

[18] E. Thonhofer, T. Palau, A. Kuhn, S. Jakubek, and M. Kozek, "Macroscopic traffic model for large scale urban traffic network design," *Simulation Modelling Practice and Theory*, vol. 80, pp. 32–49, 2018.

[19] S. Lim, H. Balakrishnan, D. Gifford, S. Madden, and D. Rus, "Stochastic motion planning and applications to traffic," *The International Journal of Robotics Research*, vol. 30, no. 6, pp. 699–712, 2011.

[20] M. Vallati, D. Magazzeni, B. De Schutter, L. Chrpa, and T. L. McCluskey, "Efficient macroscopic urban traffic models for reducing congestion: a pddl+ planning approach," in *Thirtieth AAAI Conference on Artificial Intelligence*, 2016.

[21] D. Ngoduy and D. Jia, "Multi anticipative bidirectional macroscopic traffic model considering cooperative driving strategy," *Transportmetrica B: Transport Dynamics*, vol. 5, no. 1, pp. 96–110, 2017.

[22] A. Spiliopoulou, I. Papamichail, M. Papageorgiou, Y. Tyrinopoulos, and J. Chrysoulakis, "Macroscopic traffic flow model calibration using different optimization algorithms," *Operational Research*, vol. 17, no. 1, pp. 145–164, 2017.

[23] D. Helbing, A. Hennecke, V. Shvetsov, and M. Treiber, "Micro- and macro-simulation of freeway traffic," *Mathematical and Computer Modelling*, vol. 35, no. 5, pp. 517 – 547, 2002.

[24] J. Sewall, J. van den Berg, M. Lin, and D. Manocha, "Virtualized traffic: Reconstructing traffic flows from discrete spatiotemporal data," *IEEE Transactions on Vis. and Computer Graphics*, vol. 17, no. 1, pp. 26–37, Jan 2011.

[25] M. Ben-Akiva, M. Bierlaire, H. Koutsopoulos, and R. Mishalani, "Dynamit: a simulation-based system for traffic prediction," in *DACCORD Short Term Forecasting WS*. Delft The Netherlands, 1998, pp. 1–12.

[26] W. Burghout, H. N. Koutsopoulos, and I. Andreasson, "Hybrid mesoscopic–microscopic traffic simulation," *Transp. Research Record*, vol. 1934, no. 1, pp. 218–225, 2005.

[27] M. Florian, M. Mahut, and N. Tremblay, "Application of a simulation-based dynamic traffic assignment model," *European Journal of Operational Research*, vol. 189, no. 3, pp. 1381 – 1392, 2008.

[28] T. Potuzak, "Comparison of road traffic network division based on microscopic and macroscopic simulation," in *Computer Modelling and Simulation (UKSim), 2011 UkSim 13th International Conference on*, March 2011, pp. 409–414.

[29] D. Wilkie, J. Sewall, and M. C. Lin, "Transforming gis data into functional road models for large-scale traffic simulation," *IEEE Transactions on Vis. and Computer Graphics*, vol. 18, no. 6, pp. 890–901, June 2012.

[30] A. Jamshidnejad, I. Papamichail, M. Papageorgiou, and B. De Schutter, "A mesoscopic integrated urban traffic flow-emission model," *Transp. Research Part C: Emerging Technol.*, vol. 75, pp. 45–83, 2017.

[31] W. Burghout and H. N. Koutsopoulos, *Transport Simulation – Beyond Traditional Approaches*. CRC Press, 2019, ch. Hybrid Traffic Simulation Models: Vehicle Loading at Meso-Micro Boundaries, pp. 27–41.

[32] T. D. Gillespie, *Fundamentals of vehicle dynamics*. Society of automotive engineers Warrendale, PA, 1992, vol. 400.

[33] D. Koladia, "Mathematical model to design rack and pinion ackerman steering geomtery," *International Journal of Scientific & Engineering Research*, vol. 5, no. 9, pp. 716–720, September 2014.

[34] J. M. Lucas and M. S. Saccucci, "Exponentially weighted moving average control schemes: properties and enhancements," *Technometrics*, vol. 32, no. 1, pp. 1–12, 1990.

[35] V. J. Cassol, F. P. Marson, M. Vendramini, M. Paravisi, A. L. Bicho, C. R. Jung, and S. R. Musse, "Simulation of autonomous agents using terrain reasoning," in *Proc. of the 12th IASTED International Conference on Computer Graphics and Imaging - CGIM*. Innsbruck/Austria: ACTA Press, 2011, pp. 101–108.

[36] G. Kotusevski and K. A. Hawick, "A review of traffic simulation software," *Research Letters in the Information and Mathematical Sciences*, vol. 13, pp. 35–54, 2009.

[37] U. Wilensky, "Netlogo," in *Center for Connected Learning and Computer-Based Modeling*, Evanston, IL, Northwestern University, 1999. [Online]. Available: http://ccl.northwestern.edu/netlogo/

[38] Aimsun, "Aimsun: Dynamic simulators user's manual," Accessed in nov. 2021, Barcelona, 2013. [Online]. Available: http://www.aimsun.com/

[39] P. G. GIPPS, "A behavioural car-following model for computer simulation," *Transp. Research Part B: Methodological*, vol. 15, no. 2, pp. 105–111, April 1981.